

The Kepler Mission: A Mission To Determine The Frequency Of Inner Planets Near The Habitable Zone Of A Wide Range Of Stars

W. J. Borucki and D. G. Koch

NASA Ames Research Center, M.S. 245-3, Moffett Field, CA 94035

E. W. Dunham

Lowell Observatory, 1400 W. Mars Hill Road, Flagstaff, AZ 86001

J. M. Jenkins

SETI Institute, 2035 Landings Drive, Mountain View, CA 94043

Abstract The surprising discovery of giant planets in inner orbits around solar-like stars has brought into question our understanding of the development and evolution of planetary systems, including our solar system. To make further progress, it is critical to detect and obtain data on the frequency and characteristics of Earth-class planets. The *Kepler Mission* is designed to be a quick, low-cost approach to accomplish that objective.

Transits by Earth-class planets produce a fractional change in stellar brightness of 5×10^{-5} to 40×10^{-5} lasting for 4 to 16 hours. From the period and depth of the transits, the orbit and size of the planets can be calculated. The proposed instrument is a one-meter aperture photometer with a 12° field-of-view (FOV). To obtain the required precision and to avoid interruptions caused by day-night and seasonal cycles, the photometer will be launched into a heliocentric orbit. It will continuously and simultaneously monitor the flux from 80,000 dwarf stars brighter than 14th magnitude in the Cygnus constellation.

The mission tests the hypothesis that the formation of most stars produces Earth-class planets in inner orbits. Based on this assumption and the recent observations that 2% of the stars have giant planets in inner orbits, several types of results are expected from the mission:

1. From transits of Earth-class planets, about 480 planet detections and 60 cases where two or more planets are found in the same system.
2. From transits of giant planets, about 160 detections of inner-orbit planets and 24 detections of outer-orbit planets.
3. From the phase modulation of the reflected light from giant planets, about 1400 planet detections with periods less than a week, albedos for 160 of these giant planets, and densities for seven planets.

Paper presented at : *Planets Beyond Our Solar System and Next Generation Space Missions, ASP Conf Ser* , submitted, 16-18 Oct. 1996 STScI

1. Introduction

The intense excitement of this past year surrounding the discovery of giant planets orbiting stars beyond our solar system has renewed the popular interest in the centuries old quest for other planets like our Earth. With the exception of the pulsar planets (Wolszczan 1994, Shobonova 1995), all of the planets¹ detected so far have Jovian masses (Mayor and Queloz 1995, Marcy and Butler 1996). The challenge now is to find Earth-class planets, which are 300 times less massive than Jupiter. The *Kepler Mission* is specifically designed to detect and characterize hundreds of Earth-class planets in and near the habitable zones of a wide variety of stellar types.

Detection methods capable of finding massive planets have already discovered extra-solar planets and low mass stellar companions. These techniques are expected someday to improve to the point that planets as small as Uranus can be found (ExNPS 1996). The *Kepler Mission* goes well beyond the capabilities of these methods in that it has the ability to find Earth-class planets, i.e., planets 300 times less massive than Jupiter. In addition, photometry can detect planets around all classes of stars, whereas the radial velocity method requires sufficient spectral line structure which is present only for stars less massive than F5. Astrometry and interferometry are limited to the nearest stars, which are predominately very low mass M-dwarf stars. Photometry is not subject to the background arising from local or extra-solar zodiacal light nor is it hampered by multiple component stellar systems.

We are at a singular point in history when the question of the existence of habitable worlds and life elsewhere in the Universe can be settled. Studies of stability in many-body systems indicate that most single stars, and many binary stars are expected to have planets (Lissauer 1995). The current theory for the formation of our solar system postulates that they developed from an accretion disk that formed from the collapse of a portion of a giant molecular cloud (Cameron 1988, Shu et al. 1993) and that planets form concurrently with stars. Model calculations by Lin and Bodenheimer (submitted 1996) suggest that planet formation and evolution lead to a series of planets forming and moving inward toward the central star. Only those planets survive that have not fallen into the stellar envelope at the time the disk clears. These results suggest that Earth-class planets are absent in planetary systems that have giant inner-orbit planets.

Although ground based radial velocity and astrometric techniques have detected massive planets, neither method has the sensitivity to find Earth-class planets (Black 1996); where Earth-class planets are defined to be those having masses between about 0.5 and 10 Earth masses (ExNPS 1996, p 4-1), or equivalently, radii between 0.8 and 2.2 that of Earth, R_{\oplus} . Planets of more than about ten Earth masses are not likely to be habitable because such objects can attract a hydrogen-helium atmosphere and become gas giants. On the other hand, planets less than about one half of Earth's mass that reside in or near the habitable zone are likely to lose their life-supporting atmospheres because of their low gravity and lack of plate tectonics. Although ground-based observing

¹There is also the possibility that some of these objects might be brown dwarfs or an entirely new type of object rather than planets (Black 1996). Although this distinction is important with respect to the composition and evolution of these objects, it will not be made here.

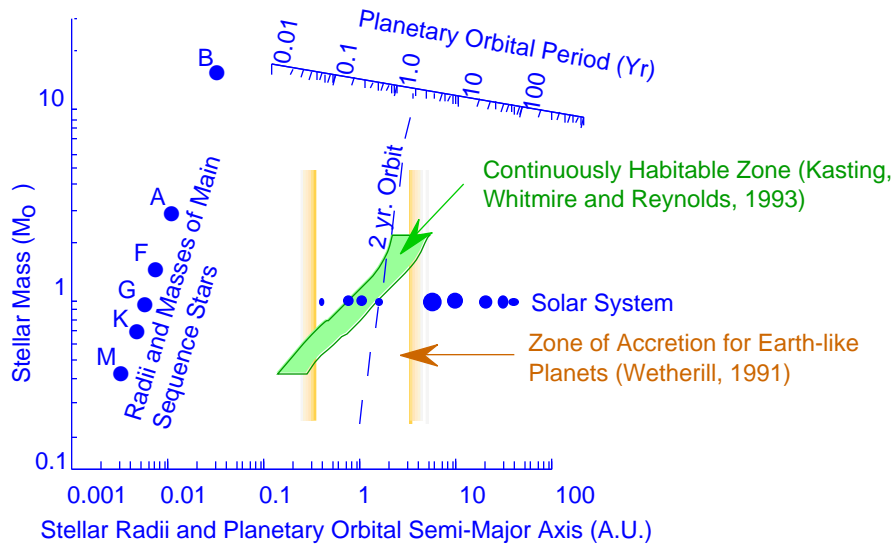


Figure 1. Relationship of Stellar Properties to the Habitable Zone and *Kepler* Search Space. Each main sequence stellar spectral type B, A, F, G, K, M is plotted to indicate the star's mass and radius on the left side of the diagram. The Habitable Zone (HZ), the planets in our solar system and the search space for the *Kepler Mission* are shown. The scale for planetary orbital periods, based on Kepler's Third Law, is also indicated.

has the sensitivity to detect micro-lensing events due to Earth-class planets, most such events will be for very low-mass stars and the planets causing the events will have such large orbital distances that they are not likely to be habitable. To find possible abodes of life, technology with the sensitivity to find Earth-class planets orbiting solar-like stars in the habitable zone is necessary.

The habitable zone (HZ) is defined by the range of distances from a star where liquid water can exist on the planet's surface and by the range of stellar types for which life has enough time to evolve, i.e., stars not more massive than spectral type A (Kasting et al. 1993). Figure 1 displays the position of the HZ for main sequence stars. According to the calculations of Wetherill (1996) rocky planets are expected to form in the region between 0.1 and 3 AU.

In this region his calculations indicate that an initial swarm of small one kilometer sized bodies placed between the star and the first giant planet collide and coalesce to form several small planets. The outer extent of the region is limited by the presence of a massive planet.

The calculations of Boss (1995) indicate that the temperatures in the inner portion of the accretion disk that formed the planets are nearly independent of the stellar mass. Therefore the inner planets should form at distances that are independent of the stellar mass and type.

We propose to search the most promising phase-space for habitable planets, that is, to search planets that are Earth-class and that have periods less than two years. In particular, the *Kepler* scientific goals are to:

1. Determine the frequency of Earth-class and larger planets in and near the habitable zone of a wide variety of stars;
2. Determine the distributions of size and radial position of these planets;
3. Estimate the frequency of planets orbiting multiple-star systems;
4. Determine the distributions of albedo, size, mass, density and radial positions of giant inner planets; and
5. Determine the properties of those stars that have planetary systems.

Some of the pertinent questions that can be addressed with the expected results of the mission are:

1. How common are planetary systems that have rocky planets in inner orbits compared to those that have giant planets within 1 AU of their star?
2. Are Earth-class planets ever found at the orbital distances observed for the giant inner planets i.e., within 0.1 AU of the star?
3. For those stars found to have giant inner planets, what fraction also have smaller planets? What are their radial distributions relative to the giant planet?
4. Are the sizes of the giant inner planets substantially larger than Jupiter as predicted in current theories (Saumon et al. 1996)? Are their atmospheres highly reflective or absorbing?
5. Do the frequency and characteristics of planetary systems depend on the stellar properties such as metallicity, spectral type, age, rotation rate, stellar activity?

2. Approach

Our approach is to use of high precision photometry to measure the periodic change in brightness of a star that occurs when a planet passes across the stellar disk, i.e., transits the star. Rosenblatt (1971), Borucki et al. (1985), and Schneider and Chevreton (1990) discuss several approaches including measuring the transit depth and the color change that occurs. The major requirement that must be met to attain the scientific goals is a multichannel photometer that can simultaneously and continuously monitor many thousands of stars with sufficient photometric precision to detect the small signals produced by transits of Earth-class planets. To meet these requirements, the *Kepler Mission* must overcome challenges in two areas:

- It must make the measurements with enough precision that signals from small planets are reliably detected with a negligible false alarm rate in the

presence of noise due to the detector, the photon flux, and stellar variability; and

- It must monitor a sufficient number of stars to obtain statistically meaningful results regardless of whether Earth-class planets are frequent or rare.

Before each of these topics is discussed in detail, it is useful to have a brief description of the proposed instrument. The *Kepler Mission* is designed to continuously and simultaneously monitor the brightnesses of 160,000 (80,000 main sequence) stars at a instrument precision of 1×10^{-5} over the several hours of a transit. The instrument will consist of a space-borne photometer with a one-meter aperture telescope, a 12° FOV, and an array of 21 CCD detectors covering the focal plane. To improve the precision and reduce saturation of the CCDs, the optical system is designed to produce large uniformly illuminated spots, rather than sharp images. The photometer will stare at a single star field throughout the mission, thus requiring minimal slewing capabilities and will have no articulated or deployable mechanisms other than a high gain antenna. The instrument will have a design life of four years and be launched on a Delta II 7425 into a heliocentric orbit.

During the operational phase of the mission, a ground-based observing program will perform spectroscopic observations to provide the spectral and luminosity classification for each star found to have a planet, so that the stellar mass, size and metallicity can be determined. These data are required to calculate the semi-major axis of the orbit and the planet's size. Radial velocity measurements will also be needed to determine the mass (or set an upper limit) of discovered large companions, so that brown dwarfs, white dwarfs, and giant planets can be distinguished. These data will also serve to delineate the structure of the planetary system by detecting giant planets not seen by transit or reflected light.

Estimation of the Number of Planets That Will Be Detected. Transits can be detected only when the planetary orbit is near the line-of-sight from the observer to the star. Geometrical considerations show that the probability of seeing a transit for randomly oriented planetary orbits is the ratio of the diameter of the star to the diameter of the planetary orbit, $d^*/2R$ (Borucki and Summers 1984). For Earth and Venus these values are 0.47% and 0.65%, respectively. Grazing transits with durations less than half that of a central transit are excluded from consideration. The usable transits account for 86.6% of the total, since a chord equal to half a stellar diameter is at a distance of 0.866 of the stellar radius. If other planetary systems are similar to our solar system in that they also contain two Earth-class planets in inner orbits and which have orbits that are not coplanar to within $d^*/2R$ (see Table 1), the probabilities can be added. Thus approximately $1.1\% \times 0.866 = 1\%$ of planetary systems like ours should show transits. *For the purpose of calculation, we assume that most main-sequence stars have planetary systems similar to ours. The observations are designed to test this hypothesis.*

One of the goals of this mission is to detect enough planets to make statistically meaningful statements about their frequency, characteristics, and association with different stellar types. Since the chance of a planetary system

Table 1 Transit Properties of Solar System Object.

Planet	Transit Depth $\times 10^{-5}$	Transit Duration t_c (hours)	Orbital Period (years)	Orbital Radius R (AU)	Geometric Probability $d^*/2R$ (%)	Inclination to Ecliptic (degrees)
Mercury	1.2	8.1	0.241	0.39	1.19	7.0
Venus	8.0	11.0	0.615	0.72	0.65	3.4
Earth	8.4	13.0	1.00	1.00	0.47	0.0
Mars	2.3	16.0	1.88	1.52	0.31	1.9
Jupiter	1000.	30.	11.86	5.2	0.089	1.3
Saturn	680.	40.	29.5	9.5	0.049	2.5
Uranus	120.	57.	84.0	19.2	0.024	0.8
Neptune	100.	71.	164.8	30.1	0.015	1.8

having the correct orbital alignment is approximately 1% for planets near the habitable zone, many thousands of stars of the desired spectral type and luminosity class must be observed simultaneously in a single field-of-view (FOV). (Continuously orienting the telescope to view fewer bright stars in many different FOVs is less efficient and increases the mission complexity and cost.) An essential constraint on the choice of a star field is that the field be far from the ecliptic plane so as not to be obscured by the Sun at any time during the year. Moreover, the payload envelope of the launch vehicle limits the pointing to within 55° of the ecliptic plane. Given these requirements, the HST Guide Star Catalog (GSC) was used to find the region of maximum star density. This was found to be centered on galactic coordinates of $(70^\circ, +5^\circ)$, RA=19h45m, Dec=+35°, in the Cygnus region. Because the star density in this field is so high, the GSC is incomplete for this region beyond visual magnitude $m_v = 12$. Therefore data from the US Naval Observatory digitization of the Palomar Observatory Sky Survey (USNO-POSS, Dave Monet, private communication), complete to $m_v=20$, was used to determine that the actual number of stars with $m_v \leq 14$ of all spectral types and luminosity classes in our FOV is 160,000.

For a system precision dominated by shot noise, there are two factors that determine if a particular planet size is detectable in transit: one is the brightness of the star (which sets the shot noise level); the other is the ratio of the size of the star to the size of the planet. The *Kepler* instrument is designed to detect a 13,000 km diameter (i.e., an Earth-sized) planet around an $m_v = 12$, G2 spectral class, main sequence star. Smaller planets can be detected around smaller or brighter stars. Larger planets can be found around larger or dimmer stars. Table 2 presents the minimum detectable planet size for a range of stellar types and brightness.

To calculate the number of stars for which a given planet size can be detected, the number of stars in each spectral type and luminosity class must be estimated. A model of the Galaxy for the selected FOV was developed using the luminosity function of Wielen, Jahreiss and Kruger (1983) (the same as that adopted by Bahcall and Soneira (B&S) (Bahcall 1986) for their galactic model), which defines the number of stars per cubic parsec (pc^3) for each absolute magnitude. The results were then normalized to the star density in the FOV from the USNO-POSS data. This provided the number of stars per apparent magnitude interval, spectral type and luminosity class. The model was cross checked against the spectral distribution of all stars with $|b| < 10^\circ$ in the catalog of *Positions and Proper Motions* (Röser and Bastian 1988), against the

Table 2 Size Dependence of Planet on Spectral Type and Magnitude

Type Area	B2	B7	A2	A7	F2	F7	G2	G7	K2	K7	M2	M8
m_v	Minimum Radius of Planet in Earth Radii											
9.0	4.00	2.64	1.71	1.37	1.20	1.02	0.85	0.75	0.67	0.56	0.43	0.09
9.5	4.03	2.66	1.72	1.38	1.21	1.03	0.86	0.75	0.67	0.57	0.43	0.09
10.0	4.08	2.70	1.74	1.40	1.22	1.05	0.87	0.76	0.68	0.58	0.43	0.09
10.5	4.16	2.75	1.77	1.42	1.25	1.07	0.89	0.78	0.69	0.58	0.44	0.09
11.0	4.27	2.82	1.82	1.46	1.28	1.10	0.91	0.80	0.71	0.60	0.45	0.09
11.5	4.42	2.93	1.89	1.52	1.33	1.14	0.95	0.83	0.73	0.62	0.46	0.09
12.0	4.65	3.07	1.99	1.60	1.40	1.20	1.00	0.87	0.77	0.65	0.49	0.10
12.5	4.94	3.27	2.12	1.70	1.50	1.28	1.07	0.93	0.82	0.69	0.51	0.10
13.0	5.33	3.53	2.28	1.84	1.62	1.38	1.15	1.00	0.88	0.74	0.55	0.11
13.5	5.80	3.84	2.49	2.00	1.77	1.51	1.26	1.09	0.96	0.80	0.60	0.12
14.0	6.38	4.23	2.74	2.21	1.94	1.66	1.38	1.20	1.05	0.88	0.66	0.13
	giant planets		planetary cores		habitable planets, $M \leq 10$				$M < \text{Earth size}$			

distribution of dwarfs to giants of the B&S model and the number of M-dwarfs in the *Catalog of Nearby Stars* (Gliese and Jahreiss 1991). This stellar distribution was convolved with the minimum size information from Table 2 to yield the number of main sequence stars of each spectral type for which a given planet size can be seen. This result is shown in Figure 2a. The total number of stars in the FOV for which each planet size can be detected is shown in Figure 2b. Assuming a 1% detection probability for planets in the habitable zone, 570 Earth-sized planets should be detected if there were no loss due to the presence of binary stars in the FOV. (However, see the next paragraph.)

About half of the stars monitored are likely to be multiple systems. Numerical integrations have shown that there is a range of orbital radii for which stable orbits are not possible. (Black and Pendleton 1983, Dvorak et al. 1989, Donnison and Mikulskis 1992). Based on an analysis of observed binary systems from Heacox and Gathright (1994), we estimate that 23% of the total binary population of stars cannot have planets in stable orbits with radii between 0.4 and 2 AU. Further, if the brightnesses of both stars are similar, then the signal to noise ratio (SNR) of a transit will be approximately one-half that for a transit occurring in a single-star stellar system and the transits will be difficult to detect. Based on the brightness distribution of companions to G dwarfs in binary stars tabulated by Duquennoy and Mayor (1991), we determined the fraction of G-dwarf binaries whose companions are dim enough not to appreciably degrade the SNR by more than 20%, thus allowing detection of transits with the *Kepler* photometer. Accounting for these fractions and the fact that radial velocity observations have already shown the presence of planets orbiting individual stars in multiple stars systems (Cochran et al. 1996), the fraction of suitable binary star systems is expected to be 0.68. This is sufficiently large that the frequency and distribution of planets in binaries can be established. The fraction of the stellar population for which planets can be detected is estimated to be $0.5 + 0.68 \times 0.5 = 0.84$. Hence, 480 Earth-class planets should be detected after accounting for the presence of binary star systems. (A more detailed discussion of these calculations is presented in Borucki et al. 1997).

When a planetary system with small relative orbital inclinations is viewed near the intersection of the orbital planes of two planets, both planets can be detected. For systems having similar spacing and inclinations as

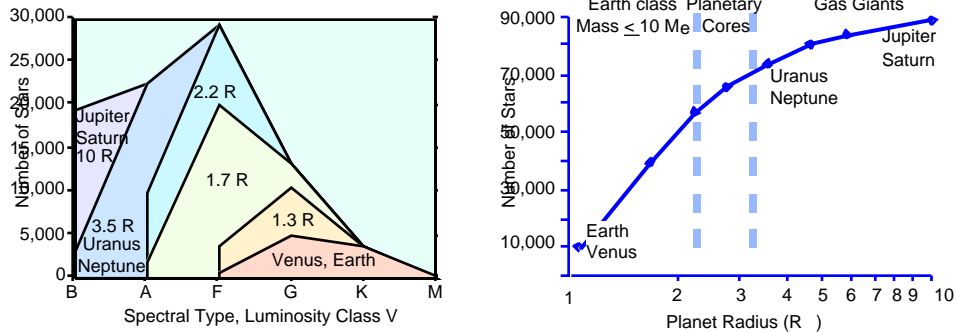


Figure 2a and 2b. The number of dwarf stars in the selected FOV for which a given planet size can be detected. The figure on the left shows the number for each spectral type and that on the right shows the total number as a function of planet size.

the Venus-Earth or Earth-Mars combinations, the chance of observing both planets is approximately 12% (Koch and Borucki 1994). Consequently about 60 of the discovered systems should show more than one planet.

Eclipsing binary stars in the survey represent an opportunity to determine if planetary orbital plane is coincident with the stellar orbital plane. Although the transit signatures will not be as simple as for single stars, they can be recognized (Jenkins et al. 1996) and their characteristics used to determine the orbital eccentricity of the planet's orbit (Bell and Borucki 1995).

Photometric precision required to detect Earth-class planets. Table 1 shows that signal levels will range from 3×10^{-5} for a Mars-sized transit to 8.4×10^{-5} for an Earth-sized planet transiting a solar-like star. However planets with radii as large as 2.2 times that of the Earth might not be so massive that they attract a massive hydrogen-helium atmosphere and become gas giants. Thus signal levels as high as 4.1×10^{-4} can be expected from Earth-class planets orbiting solar-like stars. Signal levels substantially larger and smaller can be expected from smaller and larger stars, respectively. It will be shown later that a total SNR of approximately eight (or more) from a series of transits is needed to unambiguously recognize a planetary transit when many stars are monitored. For a four year mission that searches for planets with periods near one year, this requirement translates to a SNR of four per individual transit. Thus to obtain a SNR of four when the signal level is 8.4×10^{-5} requires that the measurement precision be about 2×10^{-5} . For observations made in the Earth's atmosphere, the varying levels of dust, haze, and clouds cause changes in the apparent brightness and color of the stars. Based on observations with a world-wide network of large telescopes, Gilliland et al. (1993) found that the best obtainable precision for ground-based observations at the time scales commensurate with transit durations is about 8×10^{-4} even when extreme measures are taken to minimize the effects of atmospheric fluctuations. Thus, to avoid the transparency and refractivity fluctuations caused by the Earth's atmosphere and the disruptive effects of day-night and seasonal cycles, observations must be made from a space-borne platform. Even for a space-borne photometer there are noise

sources, such as, photon shot noise, detector noise, pointing jitter and stellar variability. However, in contrast to typical astronomical photometry, there are no requirements for a standard passband, long-term accuracy, or comparison of widely separated stars. The only requirement is to detect the change in brightness of a given star, by whatever means, over the duration of a single transit. Consequently, common ground-based observing with CCD photometry is not a useful intuitive guide.

System precision is defined to include all noise sources. It is the pertinent value to use when calculating the SNR for a transit by a planet of a given size for an individual star. Because system precision includes both the shot noise and the stellar variability, it is a function of the star's apparent magnitude and its variability. In practice, the noise level is derived from observations of each star. The minimally-acceptable SNR is set by the requirement that no more than one false alarm occur for the entire mission. Thus the smallest planet that can be detected around an individual star depends on the noise level of that star; i.e., the system precision.

To obtain a system precision of 2×10^{-5} , the sum (in quadrature) of the noise introduced by stellar variability, shot noise, and the instrument itself must be less than or equal to this value. To minimize mission costs while meeting the mission objectives, the system has been designed to produce a shot-noise of about 1.4×10^{-5} for integration periods commensurate with transit durations for a $m_V = 12$, G2, star by using a combination of a sufficiently large aperture and high efficiency back-illuminated CCD detectors. Specifically, it has been designed to collect 5×10^9 photoelectrons for a $m_V = 12$ star in five hours. (Note that most transits of by planets in 1 AU orbits around a solar-like star will have durations more than double this value and therefore will collect more than double this value of photoelectrons.) At frequencies pertinent to the detection of transits, the noise introduced by stellar variability for solar-like stars is expected to be similar to that measured for the Sun, i.e., 1×10^{-5} . (See discussion below.) Therefore to obtain a system precision of 2×10^{-5} the instrument should have a precision near 1×10^{-5} .

Instrument Precision. Although detection of transit signals from Earth-size planets requires an instrument precision of order one part in 10^5 , this is intrinsically much easier than the one part in 10^8 routinely obtained by the Doppler velocity technique that has produced the majority of planetary discoveries. Nevertheless, it is important to demonstrate that the photometric approach can meet this requirement and all the technical challenges imposed by the scientific objectives. The instrument precision includes all the types of noise introduced by the detector and the instrument, such as the noise induced by jitter in the telescope tracking. To demonstrate that CCDs can attain a precision of this level, laboratory tests of both front- and back-illuminated CCDs were performed at Lick Observatory and NASA Ames Research Center. With sufficient thermal, mechanical and voltage stability, and with correction of image motion and amplifier non-linearity, near shot-noise limited performance of better than 1×10^{-5} was repeatedly demonstrated with flux levels and over time periods commensurate with transits (Robinson et al. 1995; Jenkins et al. 1996, 1997-this issue). The techniques used to attain this level of photometric precision include:

1. Relative photometry: The brightness of each target star is divided by the average of all the stars on each quadrant of each CCD every 3 s to reduce sensitivity to time dependent gain variations;
2. Defocused star images: Each image is defocused to cover a 7x7 pixel area. This reduces the CCD sensitivity to motions, pixel-to-pixel variations, and mitigates saturation problems.
3. Only short term precision required: Transit durations are a few hours to less than a day. There is no need for long term precision.
4. Star images fixed on the same pixels: This reduces brightness variations induced by pixel-to-pixel variations and photometer motions.
5. Operate the CCDs near full well capacity and at low temperature: These conditions reduce read noise and dark current to negligible levels.
6. Operate in stable thermal and scattered light background: Choose a heliocentric orbit.

Other factors that limit the attainable photometric precision include star field crowding, shutterless operation of the system, cosmic ray events, and slow degradation of CCD performance due to radiation. Table 3 presents several noise sources and their effect on photometric precision. For reference, the minimum number of photo-electrons produced by the signal is also listed.

Note that photoelectron shot noise and dark current obey Poisson statistics; if N electrons are integrated, the fractional precision is $1/\sqrt{N}$. Read noise scales with the square root of the number of pixels (49) and the number of readouts (6000) in a five hour integration. No corrections or calibrations are needed to reach the read noise and shot noise figures given in Table 3. The value of the dark current is given for the end-of-mission time after degradation from a four year exposure to energetic particle bombardment expected from the solar proton events and galactic cosmic rays. It is clear from Table 3 that shot noise dominates other noise sources. While no obvious physical effect should prevent CCDs from reaching the required level of precision, there is concern for the effect of non-uniformity, both from pixel to pixel and within a pixel (Jordan et al. 1994). Accordingly, independent groups at Lick Observatory, Ball Aerospace, and NASA Ames Research Center conducted tests of precision achievable with CCDs in laboratory experiments simulating the conditions for the *Kepler Mission*. The results of these experiments (Robinson et al. 1995, Jenkins et al. 1996, 1997) indicate that both front- and back-illuminated CCDs are nearly shot-noise limited detectors at the precision level required for the *Kepler Mission*. However, the protocols listed earlier must be observed and the observed image motion must be compensated. Previous results (Robinson et al. 1995) dealt with front-illuminated CCDs where the image is imposed on the electrical traces covering the silicon substrate. Because back-illuminated CCDs impose the image on the other side, they have a higher quantum efficiency and are expected to have much lower sensitivity to image motions. Although more difficult to manufacture because the supporting substrate must be chemically etched away, they are the

Table 3. Noise Sources and Their Expected Contribution to the Noise Budget

Requirement	Value at 5 hours	Induced Fractional Noise for 5 hr Integration		
		$m_v=10$	$m_v=12$	$m_v=14$
Signal(e^-)		3.2×10^{10}	5.1×10^9	8.1×10^8
Shot Noise from Signal		5.6×10^{-6}	1.4×10^{-5}	3.5×10^{-5}
Dark Current $<100 e^-/p/s$ ¹	9,400	2.9×10^{-7}	1.8×10^{-6}	1.2×10^{-5}
Read Noise $<50 e^-/p$	8,130	2.5×10^{-7}	1.6×10^{-6}	1.0×10^{-5}
Pointing Noise		$<5.0 \times 10^{-6}$	$<5.0 \times 10^{-6}$	$<5.0 \times 10^{-6}$
Stellar Variability		1.0×10^{-5}	1.0×10^{-5}	1.0×10^{-5}
Instrument Noise (measured) ²		1.0×10^{-5}	1.0×10^{-5}	1.0×10^{-5}
TOTAL SYSTEM NOISE		1.5×10^{-5}	2.0×10^{-5}	3.8×10^{-5}
Transit SNR () ³		5.3	4.0	2.1

¹ Dark current is for end-of-life after four years of energetic particle bombardment. See text.

² Includes noise from dark current, read, pointing, and undetermined sources.

³ SNR=Transit signal from Earth-size planet crossing a solar-like star divided by the Total System Noise

detectors of choice when operated at the requisite precision. To verify the performance of this type of detector, several tests were carried out by focussing arrays of simulated star images on a Reticon back-illuminated CCD. Measurements were made to determine the sensitivity to motion at the milli-pixel level and at much larger levels. As expected, the sensitivity to motions was reduced from that for front-illuminated CCDs. Tests demonstrated that a precision of a few parts per million are readily attained. A complete discussion is presented by Jenkins et al., this issue.

Star field crowding affects the precision when the defocused images of dim stars overlap those of target stars. Based on the known number of stars in the FOV, target star images occupy approximately 8% of the focal plane and stars with $m_v \leq 16$ occupy roughly half of the focal plane. For a 16th magnitude star image that overlaps that of a 14th magnitude target star, the shot noise increases by 8% and the depth of a transit across the target star decreases by about 15% (a small and calibrated amount). For brighter target stars the effects are negligible. If the background star is variable with a relatively large amplitude, its variability adds to the variability of the target star. Variability with periods substantially different than the transit periods is not a significant problem, so most classes of variability, regardless of amplitude, do not cause difficulty. The most likely source of confusion is that due to stars having transits by giant planets. There will be about 300,000 stars with $m_v > 16$ in the 7×7 apertures of the 160,000 target stars. Of these, half will be main sequence stars, and of these, as many as 0.5% might have a transiting giant planet in a terrestrial-size orbit with the proper orientation to show a transit. Therefore, it is possible that up to 750 additional planet detections from planets at least as large as Neptune

orbiting dim background stars will be found in overlapping star images. In 80% of these cases, the star image centers will be more than two pixels apart, permitting identification of the actual star undergoing transit. Ground-based observations can further reduce the uncertainty in those cases where the target and background stars' overlap is too great to be handled with *Kepler*.

The 21 CCDs flown on *Kepler* will be subject to solar flares and cosmic rays. Experiments carried out by our industrial partner (Ball Aerospace, Boulder, CO) with the AXAF star tracker CCDs indicate that the major effect of radiation damage over the lifetime of the *Kepler Mission* will be an increase in dark current from an initial level of 10 e-/s/pixel to 100 e-/sec/pixel at the end of the mission lifetime. Increases in dark current will occur during the six major (but brief) solar flare events expected during the mission. The main effect will be to change the apparent transit depth slightly. Between flares, the dark current is expected to be nearly constant. A secondary effect of lower charge transfer efficiency is of no consequence for *Kepler* because of the defocused images and very high signal levels. These laboratory measurements and calculations demonstrate the proposed *Kepler* system can meet the photometric precision requirements with commercially available CCDs. The required technology is already in hand to detect Earth-class planets. Next we discuss stellar variability and show that, unless it is much larger than exhibited by the Sun, it will not prevent the detection of Earth-size planets.

Stellar Variability. The stellar variability on a time scale of several hours is too small to be measured by even the best ground-based systems because of atmospheric scintillation, transparency fluctuations, and day/night cycles (see the earlier discussion). Only data for the Sun obtained from radiometers aboard the Solar Maximum Mission (SMM) satellite and Solar and Heliospheric Observatory have the required precision (Fröhlich 1987, and Willson and Hudson 1991). These data show that the solar variability is about 1×10^{-5} on a time scale of several hours and can be further reduced by excluding the highly-variable UV portion of the spectrum. The results of the Active Cavity Radiometer for Irradiance Monitoring (ACRIM 1) aboard the SMM satellite were used to model the expected stellar variability. This instrument measured the total solar flux over all wavelengths (Willson et al. 1981). The data were obtained directly from R. Willson and spanned 4.5 years, from 1985 (near solar minimum) into 1989 (near solar maximum). This is the only published data set on any star with the precision required for evaluating the performance of the *Kepler Mission*. Because the ACRIM 1 instrument included the UV portion of the spectrum, these data are expected to be 30% more variable than the *Kepler* measurements. The data were bin-averaged to 1.56 hr resolution to mitigate the effects of data gaps caused by the low-Earth orbit of SMM and to decrease small systematic errors introduced by the corrections made for the satellite's orbital motion. A statistical analysis demonstrated that solar variability is well-modeled as a Gaussian noise process. Figure 3 shows the power spectra measured when photon shot noise has been added corresponding to that expected for stars with $m_V = 10, 12$ and 14. Most power in the measurement noise occurs at periods greater than ten days, corresponding to the rotation of sunspot groups and solar-cycle time-scale variations (Fröhlich 1987). The steep slope at ten days extending to two days is

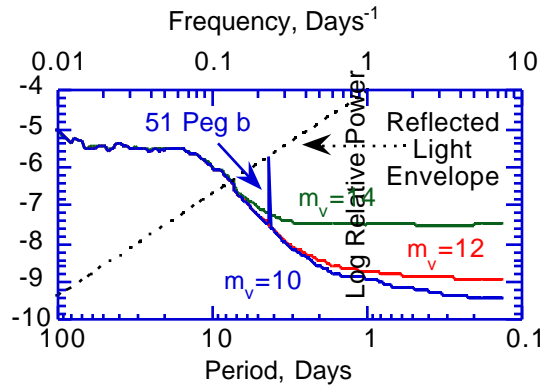


Figure 3. Power Spectral Density (PSD) for Measurement Noise, Transit and Reflected-Light Signals. Measurement noise including stellar variability, shot noise, and pointing noise appropriate for $m_v = 10, 12,$ and 14 stars are shown. The PSD for the reflected light from a 51 Peg-type system is shown as a diagonal line from the upper left to the lower right. This line shows how the strength of the reflected light "spike" varies with planetary period and indicates that planetary periods greater than about seven days will not be detected in reflected light.

due to solar granulation, while the shallow slope beyond this region is due to the combined effects of gravity waves (Fröhlich 1987) and the non-solar noise injected into the data set. The differences in the high frequency levels of the measurement noise are due to the varying amounts of shot noise at the different magnitudes represented.

The results presented in Figure 3 are based on the assumption that the Sun's variability will be typical of those stars in our survey. The HR-diagram has been fairly well surveyed and at this time the solar-like stars, especially the older ones with low activity, are the quietest stars known. Brightness variations with time scales greater than approximately one day will not severely reduce the detectability of transits which have durations from 4 to 16 hours. Although effects of star spots will be observed and could show brightness variations larger than those from transits by small planets, this will be a problem only for stars with short rotation periods and extensive spotting. Studies show that rotation periods increase with age (Soderblom et al. 1993) and become quite long for stars cooler than spectral type F0 (Stauffer and Hartmann, 1986). Spectral types F5 through K5 have periods of weeks, similar to that of the Sun. Consequently, the presence of star spots on these stars should not prevent the detection of planetary transits. Many stars more massive than F5 have rotation periods shorter than weeks. These stars also show much less stellar-spot activity as evidenced by their lower Ca II H and K line activity. Hence, the shorter rotation periods for these stars may not be as deleterious as for solar-like stars. Much of variability of solar-like stars occurs in the UV, which will be excluded from the measurements taken with *Kepler*. Until an instrument like *Kepler* is flown, the question of whether stars are more variable or less variable than the Sun at periods near twelve hours will remain open.

Table 4. Mean SNRs and Detection Rates for an Earth-Size Planet as a Function of Stellar Type, Magnitude, Period, and Transit Duration for 4 Years of Observation

Period (days)	Transit Duration	Number of Transits	SNR for a 1.0-R Planet			Detection Probability for a 1.0-R Planet (%)			Detection Probability for a 1.3-R Planet (%)		
			a	b	c	a	b	c	a	b	c
7	grazing	208	3.1	2.6	2.2	100	100	100	100	100	100
90	grazing	16	4.0	3.9	3.5	100	100	100	100	100	100
90	central	16	4.2	4.2	3.9	100	100	100	100	100	100
365	grazing	4	4.4	4.5	4.2	96	98	92	100	100	100
365	central	4	4.6	4.9	4.8	98	99	99	100	100	100
687	central	2	4.6	4.9	4.9	31	49	50	100	100	100

^a G0 star with $m_v = 10$

^b G5 star with $m_v = 12$

^c K5 star with $m_v = 14$

The SNR of a signal is proportional to $\sqrt{S(\nu)/W(\nu)}$, where $S(\nu)$ and $W(\nu)$ denote the power spectra of the signal and the observational noise, respectively (McDonough and Whalen, 1995). Table 4 contains SNRs for transit signals as a function of period, duration and stellar magnitude for *Kepler*. These SNRs are representative of the average over the entire solar cycle. For example, for a $m_v = 12$ solar-type star in our survey, a 12-hour transit by an Earth-size planet at 1 AU has a single-event SNR of 3.8-4.6, depending on solar activity. Once the detection threshold has been set, these SNRs can be used to determine the probability of detecting a planet transiting a particular star with a given period.

Transit and reflected light signals are well characterized, given the planetary orbital period, phase and inclination. Thus, this effort can be formulated as a classical signal detection problem in colored noise (Van Trees 1968). Once the noise is characterized, it is a straightforward task to evaluate the performance of the detector designed to yield less than one false alarm for the entire experiment, and the uncertainties in the derived planetary parameters. The detection threshold is set so that the number of independent tests to be performed times the false alarm rate of a single test is less than one. The number of independent tests depends on the signal to be detected and the range of values each signal parameter can take on. In the case of transits, there are two basic parameters: period and phase (time to first transit). For orbital periods less than two years, there are about 5×10^6 tests per star required, for a total of 8×10^{11} tests. For no more than one false alarm for the entire experiment a detection threshold of about 7 is required.

In the case of detecting non-transiting giant inner planets in reflected light, the number of tests depends only on the length of observation, which determines the spectral resolution, and the largest planetary period to be considered. Stellar variability limits this search space to periods less than seven days (see Fig. 3). Thus, there are 1,278 tests per star, for a total of 2×10^8 tests, with a requisite detection threshold of 5.7. Fig. 3 demonstrates that Jupiter-sized planets with periods less than six days are well above this threshold. These will be readily

detectable with *Kepler*. Uranus-sized planets with periods less than 2.5 days can also be detected.

The SNRs from Table 4, together with the detection threshold and the expected number of transits, were used to derive detection rates for a range of planetary periods and apparent stellar magnitudes and types. The SNR of a set of events equals the square root of the number of events times the SNR of a single event. For example, four grazing transits of a 1-R planet about a $m_V = 12$ G5 main sequence star have a combined SNR of 9, yielding a detection rate of 98%. *Kepler* will be able to detect a large fraction of 1-R planets, regardless of stellar type and apparent magnitude, and virtually all Earth-class planets with radii greater than 1.3-R. Note that planets yielding average SNRs below the threshold of 7, will be detected also, but at a lower rate than those with SNRs above 7. For example, events with SNRs of 7, 6.5, and 6, are detected 50%, 30% and 16% of the time, respectively.

Simulations were performed to demonstrate the detectability of Earth-class planets, given the expected observational noise for *Kepler*. Four 12-hr simulated transits of an Earth-sized planet in orbit about a G2 dwarf were buried in a four year noise sequence consisting of stellar variability based on the ACRIM 1 data set with shot, CCD and pointing noise added. A matched filter algorithm was applied to the data set to search for planets with periods between 100 and 400 days. Figure 4 illustrates the detectability of multiple transit events, by plotting the maximum correlation for all possible phases at each period. The peak event of 8.5, indicates a planet with the correct period of 365 days. Its presence is unmistakable and its amplitude indicates that the correlation between the matched filter and the data set would be expected to occur by chance only five times in 10^{18} independent trials. As there are only 5×10^6 tests required per star and 8×10^{11} tests for all 160,000 stars, this planet would be detected with a high confidence level.

3. Mission Description

The science objectives lead to the following mission goals:

- Brightness measurements of 160,000 stars;
- Measurements made on a time scale shorter than the transit durations;
- System precision of 2×10^{-5} for a five hours integration of a $m_V = 12$ star;
- Continuous observing over the mission lifetime; and
- Mission life of four years

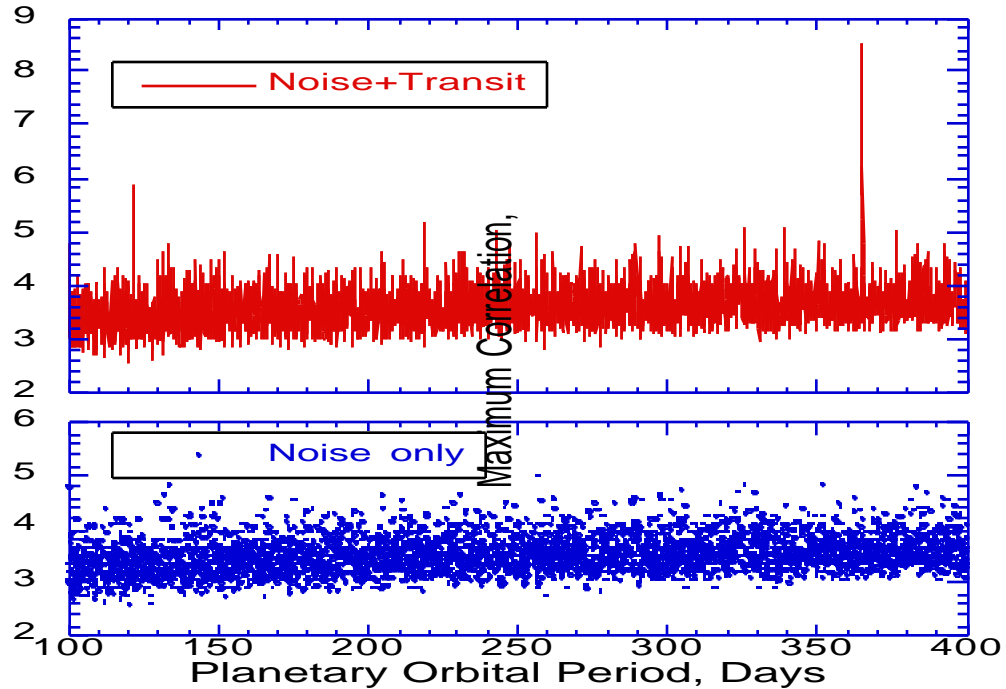


Figure 4. The upper panel shows the maximum correlation for all possible phases as a function of period for a $m_V = 12$ star transited by a one R planet. The data in the lower panel is the result for the same data when no transits are present.

These objectives define the required instrument capabilities:

- The number of stars and precision define the combination of the photometer aperture and size of the FOV for the density of stars in the field. They also define the required capabilities of the on-board processing, storage and telemetry systems.
- Mission life, continuous viewing, and a rich star field define the location of the selected star field and the orbit;
- Photometric precision and the number of stars that must be monitored define the detector selection.

The data will consist of white-light amplitude measurements over 15-minute periods with a post-calibration instrument precision of 1×10^{-5} over five hours, exclusive of shot noise and stellar variability for all stars in the 12° FOV brighter

than $m_v=14$. The system precision will be 2×10^{-5} when including shot noise for a $m_v=12$ star that has variability similar to that of the Sun near solar maximum. To detect periodic transits the mission must last long enough to detect and confirm the periodic nature of the transits. A four year mission permits a four transit detection of all orbits up to one year in length and three transit detection of periods up to 1.33 years. This duration also provides three transit detection for 50% of 1.6 yr orbits and 10% of 1.9 yr orbits.

The chosen instrument uses a modified Schmidt-design telescope to image a 12° FOV onto a focal plane consisting of twenty-one 2048×2048 pixel CCDs. The optical system is comprised of a refractive corrector, a spherical mirror, and 21 individual plano-convex field-flattening lenses; one for each CCD. Defocusing the telescope yields a uniform image size over an area of fifty pixels that permits the accumulation of a large number of photoelectrons without saturating the CCD pixels. See Figure 5 for a sketch of the optical layout. To decrease the time needed to read out each image, four readout devices are located on each CCD to read out the four quadrants in parallel. The electronic system is designed to process the output from three CCDs in parallel and then multiplex the outputs from the next group of three CCDs until all have been processed. Although this approach requires a substantial amount of electronics, the parallel design is capable of keeping up with the data stream and degrades gracefully if any component fails. Only a single number representing the measured brightness of each of the target stars at 15 minute intervals is stored for transmission to Earth. This results in an onboard data compression of 165,000 to 1.

A principal mission requirement is to continuously view the selected star field. A quantitative comparison of four candidate orbits indicated that a heliocentric orbit with a period of 372.5 days is optimum. The heliocentric orbit meets the combined Sun-Earth-Moon avoidance criteria and avoids the high radiation dosage associated with Earth orbits. There is no need for orbital maintenance negating any need for a large propulsion system and possible contamination of the sensitive optics by any propellant is eliminated. The low mass allows for the use of the lower cost Delta II 7425 launch vehicle. A second benefit of the selected orbit is that it permits the use of a simple fixed solar array design without the need for deployment or articulation. This leads to improved spacecraft pointing stability. The sunshade provides a 55° solar avoidance angle and allows for a 12.8° FOV. A one-time ejectable cover is attached to the top of the sunshade. Figure 6 provides an overall view of the proposed spacecraft and instrument.

The *Kepler Mission* has evolved from our previous FRESIP proposal (Borucki et al. 1996, and Koch et al. 1996) to the Discovery Program in 1994. The changes include:

1. The spacecraft design has been simplified by removing the propulsion stage;
2. The mass has been reduced so that a smaller launch vehicle can be used;
3. The capability of the onboard electronics has been increased so that ten times as many Earth-class planet detections are expected; and
4. The cost has been reduced and the new cost independently verified.

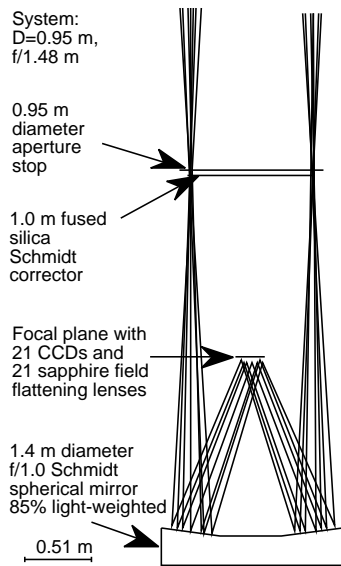


Figure 5 Optical Layout

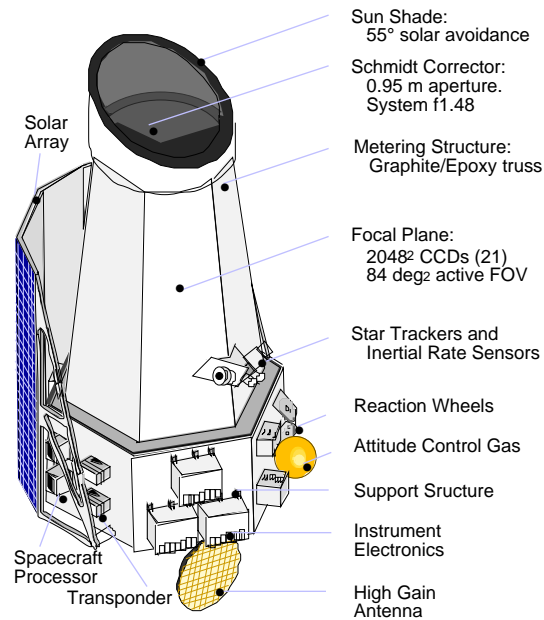


Figure 6 Kepler Spacecraft

4. Expected Results

Continuous observations of 160,000 stars at an instrument precision of 1×10^{-5} for a period of four years is expected to result in the discovery of between 1000 and 2000 planets with sizes between that of Mars to that of Jupiter around stars of spectral type M through A. Measurements of the micro variability of these stars will provide information on their rotation rates, activity cycles, surface inhomogeneities, and binary frequencies. If a selection of these stars is monitored at a higher cadence, then p-mode observations can be made to determine their age and mass (Brown and Gilliland 1994). This information and that obtained from ground-based spectroscopy should provide data needed to understand the relationship between the frequency and characteristics of planetary systems and stellar properties. (A review of other astrophysical science that can be accomplished with a high precision photometric mission is presented by Granados & Borucki 1993).

It should be recognized that the *Kepler Mission* has the capability of finding planetary systems that are much more diverse than those known. For example, if small planets exist in orbits one tenth the size of Mercury's (i.e., as small as that of 51 Peg B), then the large number of transits observed during the mission lifetime allow planets as small as Mars to be recognized around G2 dwarfs. Even smaller planets can be found around K- and M-dwarfs. If Earth-sized planets exist that orbit the massive planets observed recently, then these can be detected. If our Earth-moon system has an analog where two Earth-class planets orbit each other, that too can be recognized. In short, it is easy to speculate on a great variety of possible planetary systems. However to justify a spacecraft mission, it is necessary to demonstrate that, based on known facts, the expected results will

provide data on the variety of extant planetary systems and provide data critical to development of models of planetary system formation. Thus even unexpected results or a null result will provide useful data. The next section discusses only those results expected from the assumption that most stars have planetary systems like our solar system and on the recent discoveries that 2% of the stars have jovian mass planets in very short period orbits.

The determination of the frequency of planets can be achieved by recording data on the brightness changes of 80,000 main sequence stars of spectral types A through M and identifying transits of these stars by planets. The expected results are the detection of: 480 inner-orbit Earth-class planets, 160 inner-orbit giant planets, and 24 outer-orbit giant planets. Even a null result would be highly meaningful.

Determination of the distribution of size and radial positions planets will be achieved by measuring the brightness change of the star during the transit. For the minimally acceptable SNR of seven, the expected precision of the planetary area compared to that of the central star is about 14% implying an uncertainty in the planet's diameter of 7%. Even if as few as 5% of the target stars have Earth-class planets, the information will be of critical importance to the understanding of the structure of planetary systems.

The orbital size will be calculated from the orbital period data, the mass of the central star and Kepler's third law. Almost the entire uncertainty in the semi-major axes of the orbits will come from the mass uncertainties of the central stars which must be derived from ground-based spectroscopic observations. We estimate the mass uncertainty to be 5% from a knowledge of luminosity class, spectral type, and metallicity. Therefore, the uncertainties in the orbital radii should be about 2%.

The frequency of planets orbiting multiple-star systems will be found by comparing the number of planetary systems found in singular versus multiple star systems. Multiple-star systems can be identified from ground-based spectroscopic measurements if they are tightly bound or from high resolution or "speckle" observations if they are open systems.

The probability that a planet in a jovian-like orbit will produce a transit is only 8.9×10^{-4} (Table 1) and the chance per year of a transit occurring is 1/12th of that value. Thus the observation of 80,000 main sequence stars for four years should show transits from about 24 giant planets. These planets will have orbital periods too long to be re-observed during the mission, but individual transits will be unmistakable with a SNR of about 400 and subsequent transits will be detectable from the ground. (Detection of Neptune- and Uranus-sized planets will produce a SNR of 40 which is readily recognized with *Kepler*, but probably not by ground-based photometry.) As the identity of the star will be known, ground-based radial velocity measurements can be made to determine the orbit and mass, as there will be negligible uncertainty in the orbital inclination. Because the size will be known from the transit depth, the density of the planet can be calculated from the combination of both observations.

Recent discoveries by the radial velocity technique show that about 2% of the stars that Butler et al. (1997) monitor have giant planets with orbital periods less than one week. Because of the size of these planets and their closeness to the star, the *Kepler Mission* will readily record the modulation of the light reflected by the planets as their phases change between superior and inferior conjunction. For

periods between one and five days, the fraction of reflected light for a jovian-sized planet falls from 10^{-4} to 10^{-5} . Although these are small amplitudes, the periodic nature of the signal and the hundreds of repetitions observed during the mission allow such signals to be detected with a SNR of 6 or greater for stars no noisier than the Sun and for orbital periods less than seven days. For larger planets or quieter stars, planets with even longer periods can be detected. About 1400 giant planets are expected to be detected from reflected light given the statistical likelihood that the orbital poles of 87% of these planets will have inclinations greater than 30° . The orbital eccentricity can be found from the non-sinusoidal behavior of the waveform.

For such close-in orbits the transit alignment probability $d^*/2R$ is 10%. Hence, about 160 planets will also show transits. From the area of the planet, orbital size and the amount of reflected light, the albedos can be derived. Thus the *Kepler Mission* will provide the first information on the atmospheres of extrasolar planets.

There are about 3400 stars less massive than spectral type F5 and brighter than $m_V = 12$ in our FOV. Radial velocity observations for the 0.2% of these stars that have transits of inner giants will be carried out to determine the masses of these planets. Therefore the densities of about seven of these planets can be determined.

The properties of those stars having planetary systems can be derived from spectra obtained from the radial velocity measurements will be used to determine its spectral type, luminosity class, and metallicity. Rotation rates and stellar activity can be obtained directly from the *Kepler* observations.

5. Summary

The photometric approach is ideally suited to finding small planets in that the technology is now at hand to readily detect the small signals associated with transits. Laboratory tests demonstrate that commercially available CCDs have the required precision to detect Earth-class planets orbiting solar-like stars. Likewise, stellar variability, unless it is much larger than exhibited by the Sun, will not prevent the detection of Earth-sized planets.

In summary the expected results for a four year mission are:

1. From observation of the depth and recurrence of transits by Earth-class inner-orbit planets: The planet size and orbital radius and period for about 480 Earth-class planets in or near the habitable zone for a wide range of stars. For about 60 cases, the discovery of two or more planets in the same system.
2. From transits of giant planets: The planet size and orbital radius and period of about 160 inner-orbit planets and 24 outer-orbit planets.
3. From modulation of the reflected light of giant inner planets: about 1400 planets with periods less than one week, the albedos of about 160 giant inner-orbit planets, and the densities of seven of these planets.

References

- Bahcall, J. 1986, *ARA&A*, **24**, 577
- Bell III, J. F., & Borucki, W. J. 1995, *ASP Conf. Ser.* **74**, 165
- Black, D. & Pendleton, Y. 1983, *AJ*, **88**, 1415
- Black, D. 1996, *S&T*, **92**, 20
- Borucki, W. J., Scargle, J. D., & Hudson, H. S. 1985, *ApJ*, **291**, 852
- Borucki, W. J. & Summers, A.L. 1984, *Icarus* **58**, 121
- Borucki, W. J., Dunham, E.W., Koch, D. G., Cochran, W. D., Rose, J.A., Cullers, D. K., Granados, A., & Jenkins, J. M. 1997, *PASP*, in press
- Boss, A.P. 1995, *Science* **267**, 360
- Brown, T. & Gilliland, R. 1994, *ARA&A*, **32**, 37
- Butler, R. P, Marcy, G. W., Williams, E., Hauser, H., & Shirts, P. 1997, *APJ*, **474**, L115
- Cameron, A.G.W. 1988, *ARA&A*, **26**, 441
- Donnison, J. R. & Mikulskis, D. F. 1992, *MNRAS*, **254**, 21
- Duquennoy, A. and Mayor, M. 1991, *A&A*, **248**, 485
- Dvorak, Froeschle and Froeschle, 1989, *A&A*, **226**, 335
- ExNPS, 1996, JPL Publication 96-22
- Fröhlich C. 1987, *JGR*, **92**, 796
- Gilliland, R. L., Brown, T. M., Kjeldsen, H., McCarthy, J.K., Peri, M.L., Belmonte, J. A., Vidal, I., Cram, L.E., Palmer, J., Frandsen, S., Parthasarathy, M., Petro, L., Schneider, H., Stetson, P.B., Weiss, W.W. 1993, *AJ*, **106**, 2441
- Granados, A. & Borucki, W. 1993, NASA CP-10148
- Heacox, W. D. and Gathright, J. 1994, *AJ*, **108**, 1101
- Jenkins J.M., Doyle, L. R. , & Cullers, D. K., 1996, *Icarus* **119**, 244
- Jenkins, J., McDonald, J., Borucki, W., & Dunham, E. 1996, *BAAS* **28**, 1114
- Jenkins, J. Borucki, W., Dunham, E., and McDonald, J. 1997, this issue
- Jorden, P. R., Deltorn, J. & Oates, A. P. 1994, *SPIE* **2198**
- Kasting, J.F., Whitmire, D.P., & Reynolds, R.T. 1993, *Icarus* **101**, 108
- Koch, D., & Borucki, W. 1994, *First Int'l Conf. on Circumstellar Habitable Zones*, NASA Ames, 229
- Lissauer, J. J. 1995, *Icarus* **114**, 217
- Marcy, G. W. & Butler, R. P. 1996, *ApJ*, **464**, L147
- Mayor, M., & Queloz, D. 1995, *Nature* **378**, 355
- Robinson, L. B, M. Z. Wei, M. Z., Borucki, W. J., Dunham, E.W., Ford, C. H. & Granados, A. F. 1995, *PASP*, **107**, 1094
- Rosenblatt, F. 1971, *Icarus* **14**, 71
- Saumon, D., Hubbard, W. B., Burrows, A., Guillot, T., Lunine, J.I., & Chabrier, G. 1996, *AJ*, **460**, 993
- Schneider, J., & Chevreton, M. 1990, *A&A*, **232**, 251
- Shobanova, T. 1995, *ApJ*, **453**, 779
- Shu, F., Najita, J., Galli, D., Ostiker, E. & Lizano, S. 1993, In *Protostars and Planets III*. E. Levy and J. Lunine, Univ. of Ariz. Press
- Soderblom, D. R., Stauffer, J.R., MacGregor, K. B. & Jones, B. F. 1993, *ApJ*, **409**, 624
- Stauffer, J & Hartmann, L., 1986, *PASP*, **98**, 1233
- Wetherill, G. W. 1996, *Icarus* **119** 219

- Willson, R. C., Gulkis, S., Janssen, M., Hudson, H. S. & Chapman, G. A. 1981,**
Science, **11**, 700
- Willson R. C. & Hudson, H. S. 1991,** *Nature*, **351**, 42
- Wolszczan, A. 1994,** *Science* **264**, 538